

# Effect Modifications of Overhead-View and Eye-Level Urban Greenery on Heat–Mortality Associations: Small-Area Analyses Using Case Time Series Design and Different Greenery Measurements

Jinglu Song,<sup>1</sup> Antonio Gasparrini,<sup>2</sup> Thomas Fischer,<sup>3,4</sup> Kejia Hu,<sup>5</sup> and Yi Lu<sup>6</sup>

<sup>1</sup>Department of Urban Planning and Design, Xi'an Jiaotong-Liverpool University, Suzhou, China

<sup>2</sup>Department of Public Health, Environment and Society, London School of Hygiene and Tropical Medicine, London, UK

<sup>3</sup>Environmental Assessment and Management Research Centre, Department of Geography and Planning, School of Environmental Sciences, University of Liverpool, Liverpool, UK

<sup>4</sup>Research Unit for Environmental Sciences and Management, Faculty of Natural and Agricultural Sciences, North West University, Potchefstroom, South Africa

<sup>5</sup>Institute of Big Data in Health Science, School of Public Health, Zhejiang University, Hangzhou, China

<sup>6</sup>Department of Architecture and Civil Engineering, City University of Hong Kong, Kowloon Tong, Hong Kong, China

**BACKGROUND:** The protective effect of urban greenery on adverse heat impacts remains inconclusive. Existing inconsistent findings could be attributed to the different estimation techniques used.

**OBJECTIVES:** We investigated how effect modifications of urban greenery on heat–mortality associations vary when using different greenery measurements reflecting overhead-view and eye-level urban greenery.

**METHODS:** We collected meteorological and daily mortality data for 286 territory planning units between 2005 and 2018 in Hong Kong. Three greenery measurements were extracted for each unit: *a*) the normalized difference vegetation index (NDVI) from Landsat remote sensing images, *b*) the percentage of greenspace based on land use data, and *c*) eye-level street greenery from street view images via a deep learning technique. Time-series analyses were performed using the case time series design with a linear interaction between the temperature term and each of the three greenery measurements. Effect modifications were also estimated for different age groups, sex categories, and cause-specific diseases.

**RESULTS:** Higher mortality risks were associated with both moderate and extreme heat, with relative risks (RRs) of 1.022 (95% CI: 1.000, 1.044) and 1.045 (95% CI: 1.013, 1.079) at the 90th and 99th percentiles of temperatures relative to the minimum mortality temperature (MMT). Lower RRs were observed in greener areas whichever of the three greenery measurements was used, but the disparity of RRs between areas with low and high levels of urban greenery was more apparent when using eye-level street greenery as the index at high temperatures (99th percentile relative to MMT), with RRs for low and high levels of greenery, respectively, of 1.096 (95% CI: 1.035, 1.161) and 0.985 (95% CI: 0.920, 1.055) for NDVI ( $p = 0.0193$ ), 1.068 (95% CI: 1.021, 1.117) and 0.990 (95% CI: 0.906, 1.081) for the percentage of greenspace ( $p = 0.1338$ ), and 1.103 (95% CI: 1.034, 1.177) and 0.943 (95% CI: 0.841, 1.057) for eye-level street greenery ( $p = 0.0186$ ). Health discrepancies remained for nonaccidental mortality and cardiorespiratory diseases and were more apparent for older adults ( $\geq 65$  years of age) and females.

**DISCUSSION:** This study provides new evidence that eye-level street greenery shows stronger associations with reduced heat–mortality risks compared with overhead-view greenery based on NDVI and percentage of greenspace. The effect modification of urban greenery tends to be amplified as temperatures rise and are more apparent in older adults and females. Heat mitigation strategies and health interventions, in particular with regard to accessible and visible greenery, are needed for helping heat-sensitive subpopulation groups in coping with extreme heat. <https://doi.org/10.1289/EHP12589>

## Introduction

Climate adaptation and support of a healthy environment through nature-based solutions have been receiving increasing attention over the past few years.<sup>1</sup> A direct health impact of climate change is increased mortality risk associated with more frequent and intensive extreme heat.<sup>2–4</sup> In this context, research findings suggest that the natural environment in urban areas is intertwined with residents' health.<sup>5</sup> Urban greening connected with nature-based solutions (e.g., parks and green roofs) is increasingly seen by urban planners, policymakers, and environmental epidemiologists as being able to help limit the health impacts of extreme heat.<sup>6–8</sup> Understanding the impacts of urban greenery on heat effects can

shed light on cost-effective heat mitigation strategies and health interventions.

Despite varying definitions in the literature, urban greenery usually refers to trees and vegetation along streets, in parks, and in gardens, as well as other green spaces.<sup>9</sup> There are a number of mechanisms underlying the associations between greenery and heat–mortality effects. First, urban greenery can regulate the microclimate and mitigate urban heat through evapotranspiration<sup>10</sup> and shading.<sup>11</sup> Other pathways could also explain the health benefits conferred by urban greenery, including the reduction of air pollutants<sup>12</sup> and noise,<sup>13</sup> support of psychological recovery and stress relief,<sup>14</sup> stimulation of physical activities,<sup>15</sup> and enhancement of social cohesions.<sup>16</sup> Although the total amount of urban greenery in an area is crucial for potential heat mitigation and air filtration at the city or intra-city level, the greenness along walkable streets is more likely to improve the pedestrian summertime thermal comfort, encourage personal interactions with the natural environment, and reduce people's daily exposure to health-threatening pollutants, such as air pollution and traffic noise.<sup>17–19</sup> Given the various underlying pathways, it is important to consider diverse aspects of urban greenery and explore the potential difference in their likelihood to reduce heat effects.

A number of investigations have examined the protective effects of urban greenery from adverse heat effects.<sup>6,20,21</sup> Although most of the existing literature focuses on global and regional scales, heat mitigation strategies and health interventions are most effectively devised locally,<sup>22</sup> few studies have focused on the impacts of urban greenery on heat effects at the intra-urban level and the results vary.<sup>7,23–25</sup> The overall inconclusive findings

---

Address correspondence to Jinglu Song, Department of Urban Planning and Design, Xi'an Jiaotong-Liverpool University, 111 Renai Rd., Suzhou 215123, China. Telephone: 86-512-8188-1772. Email: [Jinglu.Song@xjtlu.edu.cn](mailto:Jinglu.Song@xjtlu.edu.cn) or [viptanghulu@hotmail.com](mailto:viptanghulu@hotmail.com)

Supplemental Material is available online (<https://doi.org/10.1289/EHP12589>).

The authors declare they have nothing to disclose.

Received 13 December 2022; Revised 30 August 2023; Accepted 5 September 2023; Published 20 September 2023.

**Note to readers with disabilities:** *EHP* strives to ensure that all journal content is accessible to all readers. However, some figures and Supplemental Material published in *EHP* articles may not conform to 508 standards due to the complexity of the information being presented. If you need assistance accessing journal content, please contact [ehpsubmissions@niehs.nih.gov](mailto:ehpsubmissions@niehs.nih.gov). Our staff will work with you to assess and meet your accessibility needs within 3 working days.

could be attributed to different measurement techniques of urban greenery. Typically, urban greenery is measured through remote sensing or land use data, such as satellite-derived index of greenness [i.e., the normalized difference vegetation index (NDVI)], the percentage of greenspace in an area based on the land use data set. However, whether such overhead-view measurement could accurately reflect what people see on the ground is questionable.<sup>26</sup> For instance, remote sensing images often fail to detect vertical green walls, vegetation covered by a bridge, or shrubs and lawns under a tree canopy.<sup>27</sup> Emerging urban big data provide an alternative way to assess urban greenery, particularly along the streets through street view services. Being a widely used service platform, Google Street View (GSV) provides panoramic streetscape images captured by cars or people walking along the streets in many cities around the world.<sup>28</sup> Recent progress in deep learning makes it possible to extract street greenery from GSV images automatically.<sup>27</sup> In this context, although street greenery has been found to be associated with better mental health,<sup>29</sup> higher rates of physical activities,<sup>30</sup> and lower mortality risk,<sup>31,32</sup> satellite-derived urban greenery has not been found to have the same effect.

What is of particular importance is that past studies mainly focused on the protective effects of overhead-view greenery against heat.<sup>20,21,23–25</sup> Less evidence has been generated for street-level visible greenery. This means that it is currently unclear whether eye-level street greenery could act as a modifier of heat–mortality associations. Even fewer studies have examined the impacts of different greenery metrics simultaneously. Although GSV images provide exciting data, a recent work showed that the GSV-derived street greenery alone may fail to capture the presence of backyards and community gardens given that their view might be blocked by buildings.<sup>33</sup> Therefore, further investigations on the effect modifications of different greenery metrics are warranted so as to understand which aspects of urban greenery can play a vital role in heat mitigation strategies. In addition, although most of the existing literature has mainly focused on the associations between urban greenery and heat effects for the general population, scant attention has been paid to the disparate health effects of urban greenery on different subpopulation groups.<sup>24,25</sup> The potential varying effect modifications of urban greenery at different levels of heat, as observed in some studies,<sup>7,34</sup> should also be noted. This

needs further examination, in particular with regard to different greenery measurements.

It is in this context that this paper aims to explore the effect modifications of urban greenery at the intra-urban level, using a recently developed case time series (CTS) design that is particularly well suited for small-area analyses.<sup>35,36</sup> With the aid of urban big data and deep learning approaches, influences of different urban greenery metrics derived from remote sensing, land use data, and street view images will subsequently be explored, including the heterogeneous protective effects of urban greenery by age groups, sex categories and across the whole range of summer temperatures.

## Methods

### Study Area and Period

Analyses were conducted at the Tertiary Planning Unit (TPU) level, the smallest planning unit of Hong Kong, with an average area of 3.88 km<sup>2</sup> and ~25,000 residents in 2016.<sup>37</sup> The analysis was restricted to the summer months, identified as the five warmest months of June to October, from 2005 to 2018. Some TPUs changed boundaries during the analysis period. This was addressed by merging adjacent TPUs with boundary changes. In total, 286 TPUs were considered in the analysis (Figure 1).

### Time-Series Data of Weather, Air Pollution, and Mortality

Data of daily mean temperature and relative humidity were obtained from the Hong Kong Headquarter station. The station was selected because it was the most representative urban station in Hong Kong.<sup>38</sup> It had a complete data set for the study period. A previous study found that the temperature–mortality associations based on this single station were similar to those based on multiple stations.<sup>39</sup>

Air pollutant data for ozone (O<sub>3</sub>) and respirable suspended particles [particulate matters with aerodynamic diameter less than or equal to 10 micrometers (PM<sub>10</sub>)] were obtained from the Hong Kong Environmental Protection Department.<sup>40</sup> Hourly monitoring data from three roadside stations were omitted from the analysis because the monitoring results were highly affected by vehicle emissions, leaving data from 11 general stations in the study for subsequent analysis.<sup>25</sup> Daily 24-h mean concentrations

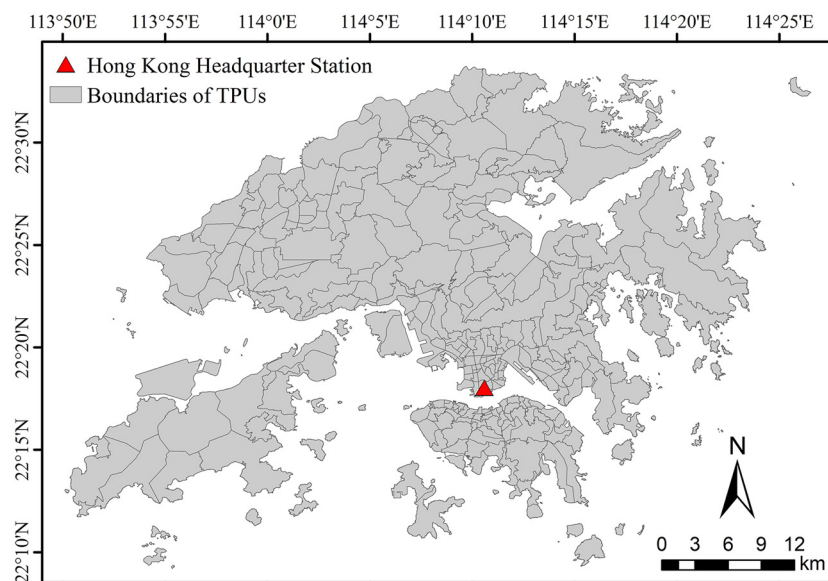


**Figure 1.** Boundaries of TPUs and the location of the Hong Kong Headquarter station. The map was created by using ArcGIS 10.5.1 (ESRI). Note: TPUs, Tertiary Planning Units.

of O<sub>3</sub> and PM<sub>10</sub> were calculated before building an average of >11 stations to represent the daily exposure levels of the population.

Time-series daily data on all-cause mortality were collected for all TPUs in Hong Kong during the summer months (June to October) from 2005 to 2018. Individual mortality data with TPU identifiers (3-digit TPU code) were obtained from the Census and Statistics Department of Hong Kong. We aggregated those data as TPU-specific daily series of total mortality counts and stratified the data by sex and age group (0–64 and ≥65 years of age) at the TPU level. In addition, causes of death were classified based on the *International Statistical Classification of Diseases and Related Health Problems, 10th Revision*<sup>41</sup> (ICD-10). In each TPU, daily counts of deaths from nonexternal causes (ICD-10 codes A00–R99) and from cardiorespiratory diseases (ICD-10 codes I00–I99 and J00–J99) were also calculated.

### Socioeconomic Data

Socioeconomic data were obtained from the 2006 and 2016 Hong Kong censuses.<sup>37,42</sup> The smallest census units with available data in the two rounds of censuses were large TPUs, in which adjacent TPUs with small populations were merged into larger units. Variables related to age, education, and income as proxy for socioeconomic status (SES) in each large TPU were identified based on a literature review.<sup>23–25</sup> This included percentages of older adults (≥65 years of age), of people >15 years of age with educational attainment only at the primary school or below, and of the working population with a monthly income below the poverty line (i.e., HKD\$2,000 in 2006 and HKD\$4,000 in 2016 according to the poverty indicator in Hong Kong).<sup>43</sup> Boundary changes were made for some large TPUs from 2006 to 2016: First, those large TPUs with boundary changes were the result of merging adjacent TPUs. Then each variable for those units was recalculated, and data for each variable over the 2-y period were averaged to reflect the SES of each large TPU during the study period. Finally, 140 large TPUs remained. The smaller TPUs within the same large TPU were assumed to have the same SES level. Pearson correlation analysis was performed between variables of SES and urban greenery measurements.

### Measurements of Urban Greenery

The study underlying this paper measured urban greenery in three distinct ways: *a*) overhead-view greenery based on NDVI, *b*) the percentage of greenspace, and *c*) eye-level street greenery derived from street view images. The NDVI is a widely used index of vegetation presence and density based on satellite images. It refers to the contrast between two bands: the near-infrared band (NIR) and the visible red band (Red). It is calculated as follows:  $NDVI = (NIR - Red) / (NIR + Red)$ .<sup>44</sup> NDVI ranges from –1 to 1, with a higher value indicating denser vegetation.<sup>45</sup> In general, a high NDVI value (0.6–0.8) corresponds to green plants (i.e., temperate and tropical rainforests), a moderate value (0.2–0.3) represents shrubs and grassland, and a very low value of NDVI (≤0.1) indicates barren areas or built-up land. A negative value represents a water body.<sup>45</sup> All available Landsat images (30 × 30 m) were collected from 2005 to 2018 and the annual NDVI composite was calculated using the maximum value compositing technique.<sup>46</sup> All Landsat images were downloaded and processed, using Google Earth Engine. After truncating the NDVI scale by setting negative values to zero, the mean NDVI value of each TPU was calculated by averaging the pixel values within the TPU boundary for each year. By averaging all annual NDVI at the TPU level for the period of 2005–2018, a single long-term average value of NDVI was produced for each TPU.

The urban greenspace data were acquired from the land utilization maps in 2006 and 2018, produced by the Hong Kong Lands Department at a 10-m resolution. This study treated woodland, shrubland, grassland, and wetland as greenspace. The greenspace data were aggregated to calculate portions of greenspace at the TPU level in each of the 2 y and were then recalculated as an average to represent the percentage of greenspace for each TPU during the study period (2005–2018).

This study measured eye-level street greenery, using GSV images. We created GSV-generating points along all streets at a uniform spacing of 50 m. Based on the coordinates of the GSV-generating points, four GSV images were downloaded for each point, constituting a panorama with a 90° field of view and north, east, south, and west headings (Figure S1A). To extract the pixels of greenery in each GSV image (Figure S1B), a separate Python script was developed using the deep learning technique of a fully convolutional neural network.<sup>47</sup> This method has been widely used in street view image processing and can accurately extract greenery pixels in GSV images after sufficient training.<sup>27,30,48,49</sup> The eye-level street greenery at each point was then assessed as the portion of greenery pixels to total pixels in the four GSV images (Equation 1), as follows:

$$\text{Street greenery (\%)} = \frac{\sum_{i=1}^4 \text{Greenery pixels}_i}{\sum_{i=1}^4 \text{Total pixels}_i} \times 100\%, \quad (1)$$

where *Greenery pixels<sub>i</sub>* represents the number of pixels representing greenery in the image *i*, and *Total pixels<sub>i</sub>* indicates the total number of pixels in that image. The values of street greenery were measured as a percentage, ranging from 0 to 100, with a higher value indicating a higher level of greenery.

To validate the results of greenery extraction, 30 GSV images were randomly selected, and greenery pixels in each image were manually extracted. A correlation coefficient of 0.91 was observed between the results of the manual extraction and those of automated greenery extraction (*p* < 0.01). The validation results aligned with those of an earlier study,<sup>47</sup> demonstrating the reliability of the methods used. Average street greenery values of all GSV points within a TPU were calculated to represent the level of street greenery in that TPU. All data processing and analyses were performed using Python scripts with GSV API.

### Statistical Analyses

The statistical analyses were conducted in two steps. During the first step, we adopted a novel CTS design that is well suited for small-scale epidemiological analysis on short-term risks associated with time-varying exposures.<sup>35</sup> The CTS design incorporates the self-matched structure in case-only models into a classical time-series form, providing a flexible and computationally efficient tool for complex longitudinal data. Unlike the original application of CTS, in which cases were represented by individual subjects,<sup>35</sup> the extended CTS were used.<sup>36</sup> This defines cases as small geographical units (i.e., TPUs). As such, the event-type outcome in the modeling framework was the daily death counts for each TPU and was associated with temperature. To simultaneously model the nonlinear and delayed effects of temperature, a bidimensional spline distributed lag nonlinear model (DLNM) was used by defining a cross-basis term.<sup>50</sup> Specifically, the bidimensional term is composed of two natural cubic splines, one for defining the exposure–response curve (two knots at the 50th and 90th percentiles of temperature distributions) and the other for modeling lag–response relationships (one knot at lag 1 over the lag period 0–3). Similar knot placements were used to those applied in a past study to

facilitate comparison across regions in different studies.<sup>36</sup> The model enforced a strict temporal control by using a TPU/year/month strata intercept, natural splines of days of the year with 4 degrees of freedom, and an interaction term with year indicators, plus indicators of days of the week and holidays, thus allowing for modeling individually varying baseline risks on top of shared long-term, seasonal, weekly trends.<sup>35</sup> The minimum mortality temperature (MMT) during the study period (June to October, from 2005 to 2018) was derived from the temperature–mortality curve and was used to center the DLNMs at the MMT as references.

In the second step, the original model was extended by introducing an interaction term to investigate the effect modifications of urban greenery measured by NDVI, percentage of greenspace, and eye-level street greenery, respectively. In particular, a linear interaction between the cross-basis temperature and each indicator of urban greenery was specified. The significance of the interaction was tested, based on the likelihood ratio test.<sup>36</sup> The relative risks (RRs) of deaths associated with summer temperatures in TPUs at a low level (5th percentile) and a high level (95th percentile) of each greenery indicator were predicted, respectively, using MMTs derived during the first stage as references. Similar thresholds were used to those applied in most recent small-area analysis studies to categorize low and high levels of urban greenery (5th and 95th percentiles of greenery indicators) to facilitate comparisons across different studies.<sup>7,51</sup>

To represent the effect modifications of urban greenery on the overall cumulative heat–mortality associations, the ratio of RRs between TPUs with a high and low value of each greenery indicator was calculated. Separate models were fitted for two age groups, young people (0–64 years of age) and older adults (≥65 years of age), for males and females, and for nonaccidental mortality and cardiorespiratory diseases to explore the age-, sex-, and cause-specific effect modifications of urban greenery based on NDVI, percentage of greenspace, and eye-level street greenery.

Finally, sensitivity analyses were conducted in the overall population and in all of the population stratifications by including daily relative humidity, O<sub>3</sub>, and PM<sub>10</sub> concentrations at 0–1 lag days to control the potential effects of other time-varying confounders.<sup>23</sup> All statistical analyses were performed, using R (version 4.0.4; R Development Core Team) with the *dlnm* package.<sup>52</sup> For all statistical tests, the significance level was set at  $p < 0.05$  (two-tailed).

## Results

During the study period (June to October, from 2005 to 2018), the average daily mean temperature was 28.0°C, ranging from 18.7°C to 32.4°C. The mean daily relative humidity was 77.78%, and the daily mean concentrations of air pollution were 41.73 μg/m<sup>3</sup> for O<sub>3</sub> and 44.69 μg/m<sup>3</sup> for PM<sub>10</sub> at 0–1 lag days. Death records without the residential location information were excluded. Thus, 221,919 deaths were included in the analysis. Nearly 80% of deaths were for persons ≥65 years of age, and 45% of deaths were by females. In total, 213,505 deaths were caused by nonaccidental diseases and 93,974 by cardiorespiratory diseases.

The descriptive statistics of urban greenery measured in three distinct ways at the TPU level are shown in Table 1. A list of the socioeconomic variables with the corresponding definition and descriptive statistics is provided in Table S1. The spatial distribution for each urban greenery measurement at the TPU level is illustrated in Figure S2, with the correlation between all variables in Figure S3. The GSV-derived eye-level street greenery was moderately correlated with NDVI (Pearson correlation  $r = 0.60$ ) and percentage of greenspace ( $r = 0.54$ ), whereas the latter two were highly correlated with each other ( $r = 0.90$ ). A weak negative correlation was observed between the percentage of older adults (≥65 years of age) and each urban greenery measurement ( $r = -0.26$  for NDVI,  $r = -0.3$  for percentage greenspace, and  $r = -0.23$  for eye-level street greenery). The other two socioeconomic variables showed no explicit association with the three urban greenery measurements.

The temperature–mortality association during the summer is represented by an overall cumulative exposure–response curve in Figure 2. The curve shows an increase in mortality risks at temperatures >25.4°C, corresponding to the MMT. Higher mortality risks were associated with both moderate and extreme heat, with RRs of 1.022 [95% confidence interval (CI): 1.000, 1.044] and 1.045 (95% CI: 1.013, 1.079) at the 90th and 99th percentiles of temperatures (30.1°C and 30.9°C) relative to the MMT. Figure 3 shows the overall cumulative temperature–mortality associations predicted for TPUs with a low (5th percentile) and a high (95th percentile) value for each indicator over the whole range of summer temperatures. We observed a significant disparity in heat effects by eye-level street greenery, as confirmed by the returned  $p = 0.032 < 0.05$  for a likelihood ratio test. However, results suggested little evidence of differential risks over the whole range of summer temperatures by the other indicators, NDVI, and percentage of greenspace, with  $p > 0.05$  (Figure 3).

Table 2 presents the RRs of TPUs at a high and low level of each urban greenery indicator at the 90th and 99th percentiles of temperatures (30.1°C and 30.9°C). Results show a significantly lower mortality risk at the 99th percentile in areas at a low level of NDVI-based urban greenery or with less eye-level street greenery ( $p < 0.05$ ), but there is little evidence of significant differentials at the 90th percentile of temperatures (30.1°C) for any indicator ( $p > 0.05$ ).

Results of the interaction term for different urban greenery measurements are illustrated in Figure 4. They are expressed as the ratio of RRs in TPUs with a low (5th percentile) and a high (95th percentile) value of each indicator over the whole range of summer temperatures. An increase in the right tail of the curves of all three indicators was observed, which is more apparent in the indicator of GSV-derived street greenery. This trend corresponds to the rapid increase in TPUs with a lack of eye-level street greenery at temperatures >30°C, as shown in Figure 3.

The age-, sex-, and cause-specific temperature–mortality associations for TPUs with a low (5th percentile) and a high (95th percentile) value of each greenery indicator are illustrated

**Table 1.** Descriptive statistics of the size and three urban greenery indicators of TPUs in Hong Kong, 2005–2018.

Indicators	Mean ± SD	Min	Percentile					Max
			5	25	50	75	95	
Area (km <sup>2</sup> )	3.88 ± 5.38	0.06	0.22	0.66	1.81	4.67	15.91	28.49
NDVI	0.46 ± 0.18	0.10	0.15	0.32	0.48	0.61	0.69	0.74
Percentage of greenspace (%)	43.98 ± 35.24	0.00	0.01	5.56	43.50	74.30	97.77	99.99
Eye-level street greenery (%)	28.56 ± 20.43	0.00	0.02	12.08	25.31	42.10	66.35	90.29

Note: The descriptive statistics include data of 286 TPUs. Max, maximum; min, minimum; NDVI, normalized difference vegetation index; SD, standard deviation; TPUs, Tertiary Planning Units.

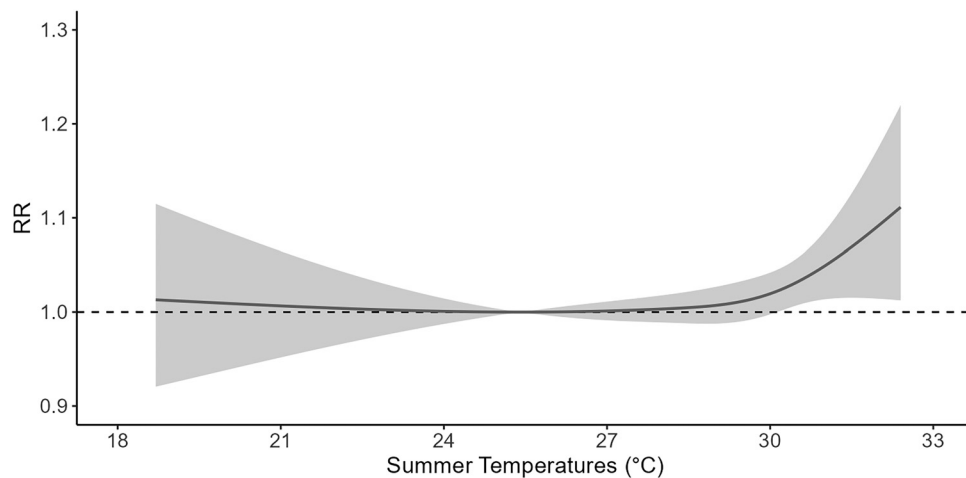


**Figure 2.** The overall cumulative exposure–response association between summer temperatures and all-cause mortality in Hong Kong, 2005–2018, with 95% confidence intervals represented by the shaded area. The analysis includes all-cause mortality data with TPU identifiers (3-digit TPU code) from June to October within the study period 2005–2018 ( $N = 221,919$ ). The estimation results were predicted by a CTS model using data aggregated at the TPU level (286 TPUs). Numeric results are included in Excel Table S1. Note: CTS, case time series; RR, relative risk; TPUs, Tertiary Planning Units.

in Figures S4–S6 and Excel Tables S4–S6. All three indicators of urban greenery were significantly associated with differential risks of summer temperatures in females. In contrast, only the eye-level street greenery retained a significant effect in older adults ( $\geq 65$  years of age) and nonaccidental mortality, as confirmed by the returned  $p$ -values of likelihood ratio tests ( $p < 0.05$ ). Both NDVI and eye-level street greenery showed significant associations with cardiorespiratory disease. However, no significant interaction was observed between urban greenery and temperature–mortality associations in males and in people 0–64 years of age ( $p > 0.05$ ). For females and older adults, a higher ratio of RRs between a high and a low value of urban greenery metrics was observed at high temperatures. The most significant increase was shown in the right tail of the curve of the GSV-derived street greenery (Figures S7 and S8). Similar trends were observed for the accidental mortality and cardiorespiratory diseases (Figures S9 and S10).

Finally, it was established that the associations between urban greenery and heat-related mortality remained even after adjusting them for other time-varying confounders (i.e., daily relative humidity and concentrations of  $O_3$  and  $PM_{10}$ ), except for the

adjustment of relative humidity in females, which rendered results nonsignificant, suggesting the robustness of the analyses (Figures S11–S14, Excel Tables S7–S10).

## Discussion

The results presented in the present paper are the first of their kind, using urban big data with deep learning techniques and the newly developed CTS design to explore the effect modifications of urban greenery on heat–mortality effects. The approach is unique in simultaneously assessing the effect modifications of different urban greenery measurements at an intra-urban level. Differential effects over the whole range of summer temperatures and by age, sex, and cause-specific mortality were also investigated.

Findings indicate significant effect modifications of eye-level street greenery on the overall temperature–mortality associations during the summer months. Little evidence of differential risks was found for urban greenery based on NDVI or percentage of greenspace. The results suggest a more apparent effect modification of urban greenery as temperatures rise, albeit not significant for some metrics. All three greenery measurements act as modifiers on the

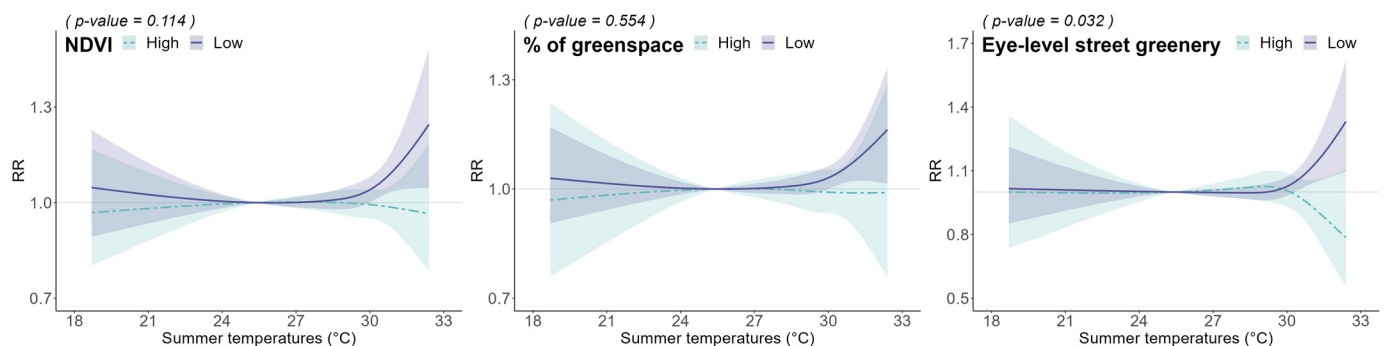


**Figure 3.** The overall cumulative exposure–response associations between summer temperatures and all-cause mortality predicted for a TPU with a low (5th percentile, solid lines in light purple) and a high (95th percentile, dashed lines in light green) value of NDVI, percentage of greenspace, and eye-level street greenery in Hong Kong, 2005–2018, with 95% confidence intervals represented by the shaded areas, and  $p$ -value for the likelihood ratio test. The corresponding values to the low (5th percentile) and high (95th percentile) levels of each urban greenery indicator are 0.15 and 0.69 for NDVI, 0.01% and 97.77% for percentage of greenspace, and 0.02% and 66.35% for the eye-level street greenery. The analysis includes all-cause mortality data with TPU identifiers (3-digit TPU code) from June to October within the study period 2005–2018 ( $N = 221,919$ ). The estimation results were predicted by an extended CTS model by specifying an interaction between the cross-basis of temperature and each urban greenery metric and using data aggregated at the TPU level (286 TPUs). Numeric results are included in Excel Table S2. Note: %, percentage; CTS, case time series; NDVI, normalized difference vegetation index; RR, relative risk; TPUs, Tertiary Planning Units.

**Table 2.** Relative risk (95% CI) for mortality associated with different levels of heat by a low (5th percentile) and a high (95th percentile) value of each urban greenery indicator and *p*-value for a likelihood test in Hong Kong, 2005–2018.

Urban greenery indicators	Level	RR for moderate heat (a T °C at P90)	RR extreme heat (a T °C at P99)
NDVI	Low	1.045 (1.005, 1.086)	1.096 (1.035, 1.161)
	High	0.993 (0.948, 1.040)	0.985 (0.920, 1.055)
	<i>p</i> -value	0.1004	0.0193
Percentage of greenspace	Low	1.034 (1.003, 1.066)	1.068 (1.021, 1.117)
	High	0.991 (0.933, 1.052)	0.990 (0.906, 1.081)
	<i>p</i> -value	0.2200	0.1338
Eye-level street greenery	Low	1.032 (0.988, 1.078)	1.103 (1.034, 1.177)
	High	1.002 (0.928, 1.083)	0.943 (0.841, 1.057)
	<i>p</i> -value	0.5209	0.0186

Note: P90 and P99 are in short of the 90th and 99th percentiles of temperature distributions (30.1°C and 30.9°C), respectively. The corresponding values to the low (5th percentile) and high (95th percentile) levels of each urban greenery indicator are 0.15 and 0.69 for NDVI, 0.01% and 97.77% for percentage of greenspace, and 0.02% and 66.35% for the eye-level street greenery. The analysis includes all-cause mortality data with TPU identifiers (3-digit TPU code) from June to October within the study period 2005–2018 (*N* = 221,919). The estimation results were predicted by an extended CTS model by specifying an interaction between the cross-basis of temperature and each urban greenery metric and using data aggregated at the TPU level (286 TPUs). CI, confidence interval; CTS, case time series; NDVI, normalized difference vegetation index; P90, 90th percentile; P99, 99th percentile; RR, relative risk; T, temperature; TPU, Tertiary Planning Unit.

temperature–mortality associations in females, whereas only eye-level street greenery works in older adults ( $\geq 65$  years of age).

In the absence of any other research, the underlying mechanisms of health benefits of the eye-level street greenery are difficult to unpick. Several plausible hypotheses may be put forward. Compared with satellite-based and Geographic Information System (GIS) measurements (i.e., NDVI, percentage of greenspace) that are typically based on the availability of urban greenery from an overhead view, GSV provides eye-level streetscape images directly matching what residents perceive when conducting outdoor activities (i.e., walking or cycling along the street). Therefore, this approach can be said to better represent how residents see and perceive urban vegetation daily.<sup>27,30</sup> In this context, our findings are comparable with those of previous works on perceived or self-reported green spaces. In a study conducted in the Barcelona Metropolitan Area, living in areas not perceived by residents to lack green spaces showed a protective effect during heat events. Similar protective effects were observed for self-reported surrounding vegetation in the past.<sup>53</sup> In contrast, lower risks were not observed in areas with a higher percentage of tree cover, which

is one of the objective GIS measurements of urban greenery.<sup>54</sup> No significant association was found between the NDVI-based greenery and a higher mortality risk during the summer months in Philadelphia, Pennsylvania, in the United States.<sup>55</sup>

The health benefits of street greenery may also be attributed to increased intermediate health-related activities, such as physical activity (i.e., walking, cycling, and other recreational physical activity)<sup>30</sup> and social interactions.<sup>56</sup> A study in Hong Kong found cycling behaviors of 5,701 residents were positively associated with GSV-derived street greenery but not with NDVI-based greenery.<sup>57</sup> Therefore, health-related activities are more likely affected by eye-level street greenery than the overhead-view greenness, which may enhance people’s general health and reduce their heat vulnerability. To reduce adverse heat effects, urban planners and policymakers may want to consider maximizing residents’ greenery exposure by increasing the accessibility and visibility of urban greenery from the pedestrian and human-scale perspectives.

For the differential heat effects by urban greenery, our results confirm the previous findings of a lower mortality risk attributable to extreme heat (at the 99th percentile of temperature distributions) in areas with a lower value of NDVI ( $p < 0.05$ ; Table 2).<sup>21,23</sup> However, there was little evidence of between-group mortality differences at moderate heat (at the 90th percentile,  $p > 0.05$ ; Table 2), which aligns with earlier intra-urban studies conducted in Seoul<sup>24</sup> and Hong Kong.<sup>25</sup> Although the existing literature largely inspects the between-group mortality differences separately at either moderate or extreme heat, few studies have simultaneously examined the differences at different heat levels and across the whole range of summer temperatures. A cohort study in three provinces in China compared heat effects between the highest and lowest NDVI quartiles and found a higher ratio of RRs at the 95th percentile of temperature [1.38 (95% CI: 0.79, 2.42)] than at the 75th percentile [1.06 (95% CI: 0.85, 1.31)], albeit with overlapping confidence intervals.<sup>8</sup> In the French cities of Paris and Rouen (Petite Couronne), the ratio of RRs between municipalities with a low and a high level (at the 5th and 95th percentiles) of green spaces or trees were found to increase with rising temperatures.<sup>7</sup> The findings presented above are consistent with those results, showing a more apparent health discrepancy by urban greenery as temperature rises, albeit not significant for some measurements (Table 2, Figure 4). Our investigation can further calculate the impacts on a smaller scale (intra-urban level) and compare the effect modifications of different urban greenery measurements. No

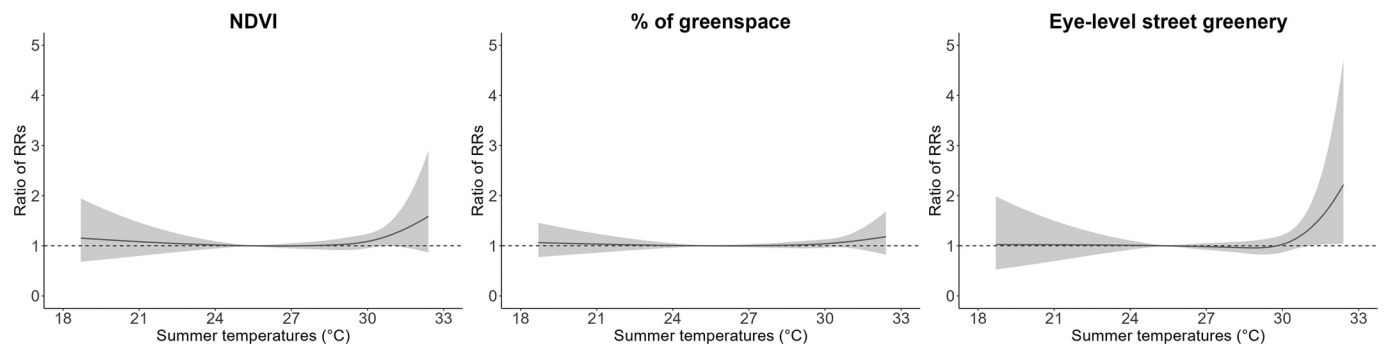


**Figure 4.** The estimated interactions between urban greenery and the overall cumulative heat–mortality associations at summer temperatures, expressed by the ratio of RRs between TPUs with a low (5th percentile) and a high (95th percentile) value of NDVI, percentage of greenspace, and eye-level street greenery in Hong Kong, 2005–2018, with 95% confidence intervals represented by the shaded areas. The corresponding values to the low (5th percentile) and high (95th percentile) levels of each urban greenery indicator are 0.15 and 0.69 for NDVI, 0.01% and 97.77% for percentage of greenspace, and 0.02% and 66.35% for the eye-level street greenery. The analysis includes all-cause mortality data with TPU identifiers (3-digit TPU code) from June to October within the study period 2005–2018 (*N* = 221,919). The estimation results were predicted by an extended CTS model by specifying an interaction between the cross-basis of temperature and each urban greenery metric and using data aggregated at the TPU level (286 TPUs). Numeric results are included in Excel Table S3. Note: CTS, case time series; NDVI, normalized difference vegetation index; RRs, relative risks; TPUs, Tertiary Planning Units.

studies were identified that investigated indicators that can be compared with our “eye-level street greenery” indicator derived from GSV imagery. Future studies are thus warranted to generalize our findings to other cities with different socioeconomic and climate characteristics.

Owing to a lack of scientific evidence, the exact mechanism for more apparent effect modifications of urban greenery at high temperatures cannot be fully elucidated. Potential explanations may stem from several pathways by which urban greenery confers health benefits. First, vegetation accelerates evapotranspiration at high temperatures to regulate the microclimate,<sup>58</sup> leading to amplified cooling effects for residents living in greener areas. Second, high temperatures may discourage people’s outdoor activities in greener areas, as observed in a recent study in India.<sup>59</sup> Therefore, residents living in areas with a high level of urban greenery are less likely to suffer adverse heat impacts, especially during extreme heat.

Significant effect modifications were observed of eye-level street greenery in older adults ( $\geq 65$  years of age) but no significant results were found for other people (0–64 years of age). The age discrepancy may be due to several pathways. First, given that older adults mainly conduct their daily activities in areas close to their residential addresses, urban greenery within or near their residential areas is a more critical greenery exposure context.<sup>60–62</sup> In Hong Kong, most younger people have a separation between work and residence (about 82.6%).<sup>37</sup> They may spend less time at their residential address, reducing their health benefit from urban greenery around their residential areas. Second, although almost all heat-adaptation strategies appear to be underused by older adults, younger people tend to engage in more heat-adaptive behaviors, such as turning fans on with the windows opened, changing clothes, taking a shower, or leaving the house.<sup>63</sup> As such, the effect modifications of urban greenery on young people’s heat hazards might be weakened. The finding also confirms the hypothesis of the “equigenesis” theory in which disadvantaged groups of people are likely to benefit more from urban greenery because they tend to lack access to other health-promoting resources, leading to a higher dependency on proximate greenspace.<sup>64</sup>

Effect modification of eye-level urban greenery was found to have a tendency to be pronounced at high temperatures, leading to significant variations in mortality risks under extreme heat in older adults ( $\geq 65$  years of age). The findings are timely in generating evidence on the foreseeable health benefits of urban greenery, particularly in the face of rapid aging and global warming. In Hong Kong, the percentage of older adults ( $\geq 65$  years of age) is projected to increase from 17.6% in 2019 to 26.2% in 2029,<sup>65</sup> whereas the frequency of extreme heat (days with temperatures above the 99th percentile) in the future (2074–2099) is projected to be 10.23 times that of the average of historical period (1980–2005) under high emission scenarios [e.g., Representative Concentration Pathway 9.5 (RCP8.5)].<sup>66</sup> Identifying what category and strategic locations of urban greenery could contribute to cost-effective implementations of heat mitigation strategies and to maximize the health benefits to heat-sensitive subpopulations. In this context, our study marks a starting point for future work and relates to climate action plans in coping with future population aging.

Females are likely to benefit more from exposure to urban greenery in hot seasons. Traditionally, females spend more time around their residential areas performing domestic tasks, which exposes them to more residential greenery.<sup>67</sup> Area-level measurements of urban greenery around residential addresses would thus be a better approximation of the daily exposure of females than males. An increase in heat-related morbidity and mortality among people with known mental health problems has also been reported.<sup>68</sup> Given that more pronounced mental health benefits

of surrounding urban greenery and self-report greenery were observed in females than males,<sup>69</sup> females may have a higher dependency on urban greenery in coping with heat stress. The existing literature also indicates a generally higher risk estimate for heat among females.<sup>70</sup> As climate change threatens to widen existing sex-based health disparities,<sup>71,72</sup> policymakers and urban planners are suggested to develop sex-specific heat mitigation strategies, for which our findings may provide practical implications related to urban greenery interventions.

Our study is among the first intra-urban studies that conducted small-area analyses with street view greenery data in the context of heat-health impacts. A methodological strength is the way in which the eye-level street greenery was estimated, namely, by coupling cutting-edge deep learning with street view data. Although earlier studies focused on satellite-based or GIS metrics (i.e., NDVI and percentage of greenspace) that typically capture urban greenery provision from an overhead view,<sup>6,7,23</sup> we further examined the potential effect modifications of eye-level street greenery derived from GSV imagery. Connected with this, testing multiple urban greenery metrics simultaneously is a particular strength of our study. Other works exploring urban greenery often rely on a single metric, producing contradictory results. However, different measurements capture diverse aspects of urban greenery and differ in their underlying pathways.<sup>73</sup> In addition, using the CTS design made it possible to quantify heat effects using small-scale attributes and to identify potential modifiers of heat–mortality associations that would otherwise be masked at lower resolutions.<sup>74</sup> Our study went beyond the existing research by observing the more apparent effect modifications of eye-level street greenery on heat effects and a pronounced protective effect of urban greenery as temperatures rise. Furthermore, our findings provide additional evidence for the health benefits of urban greenery to heat-sensitive subpopulations; namely, older adults ( $\geq 65$  years of age) and females. In facing population aging and global warming, these findings can provide a scientific basis for age- and sex-specific urban greenery interventions and inform cost-effective implementations of heat mitigation strategies.

Several limitations should be acknowledged. First, although the CTS methodology is well suited to analyzing small-area data, it still uses aggregated data and is potentially susceptible to the “ecological fallacy.”<sup>36</sup> The impact of the size of TPUs on aggregation of urban greenery indicators needs further investigation.<sup>75</sup>

Second, there were no home addresses of each death owing to privacy issues and, therefore, greenery near people’s homes could not be assessed, although the greenery likely varies even within fine-scale units. This limitation provides key insights for future studies on data of health outcomes at the individual level.<sup>76,77</sup>

Third, single sources of air temperatures might be a limitation for small-area analyses. Even though the between-area variation is likely smaller when compared with the temporal variation of air temperature, thus probably introducing nondifferential estimation results, the use of high-resolution temperature data is expected to result in more precise estimates.<sup>36</sup> Further studies are thus warranted to address this issue if high-resolution temperature data are available.

Fourth, neither eye-level street greenery nor satellite-derived (i.e., NDVI) or GIS metrics convey the full spectrum of characteristics of greenery, such as the vegetation type, the size and shape of greenspace, and the greenery quality. However, different vegetation types and settings are likely to have differential effects on heat–mortality associations.<sup>78</sup> Not all greenery measurements reflect the actual visit or use of greenery. Therefore, our exposure assessment may be biased.<sup>79,80</sup> Recent work on new data and metrics of greenery exposure also provide avenues of future studies on the impact of using different satellite images,<sup>75</sup> and the use of different satellite-derived metrics of urban greenery.<sup>81</sup>

Fifth, it is unavoidable that the assessment of eye-level street greenery may be affected by the availability of GSV images. As such, images are mainly taken by moving vehicles, and greenery far from roads is usually not included.<sup>82</sup> The assessment of eye-level street greenery in areas inaccessible to vehicles may be inaccurate. In addition, because the effect estimates were computed over a relatively long study period, potential temporal variations in some urban greenery metrics were not accounted for, such as the percentage of urban greenery and eye-level street greenery. This limitation also provides fertile ground for continued work on the temporal changes of the effect modifications of urban greenery on heat–health associations if data are available. Moreover, this study derived risks at different levels of urban greenery by using univariate models, thus not accounting for other factors that might partially explain differences in the heat–mortality associations within typologies (e.g., by the SES, by air pollution levels). However, the weak correlations between indicators of SES and urban greenery shown in Figure S3 indicate the confounding effects of the former would be, if present, minimal to the latter. The role of air pollution concentrations as confounding variables remain debated.<sup>83</sup> Nevertheless, continued work on more advanced models are warranted to disentangle the effect modifications of different variables. Last, the associations between urban greenery and other heat–health outcomes, such as morbidity outcomes (e.g., hospitalization, emergency department visits) should be further investigated.

## Conclusions

This paper reported on a small-area analysis of the effect modifications of urban greenery on the heat–mortality associations in Hong Kong from 2005 to 2018, based on an extended CTS design. The analyses measured urban greenery in three distinct ways, based on urban big data and deep learning approaches, comparing the effect modifications of different urban greenery measurements, namely, NDVI, percentage of greenspace, and GSV-derived street greenery. The differential in the heat–mortality effects by urban greenery was also examined for different age and sex groups, cause-specific mortality, and at different levels of heat. The findings of more apparent health benefits of eye-level street greenery against heat effects can be used to inform cost-effective heat mitigation policies with targeted urban greening interventions. The pronounced influences of urban greenery at high temperatures on older adults ( $\geq 65$  years of age) and females can provide a scientific basis for climate action plans in coping with global warming and population aging in the future.

## Acknowledgments

Contributions of the authors were as follows: J.S.: conceptualization, methodology, data curation, software, formal analysis, writing-original draft, writing-review and editing, funding acquisition; A.G.: methodology, software, writing-review and editing, funding acquisition; T.F.: writing-review and editing; K.H.: data curation, funding acquisition; and Y.L.: data curation, writing-review and editing, funding acquisition.

We thank the Hong Kong Census and Statistics Department for its efforts in collecting and processing the census and mortality data.

The study was supported by the National Natural Science Foundation of China (grants 42007421, to J.S., and 42001013, to K.H.), General Research Project Fund of Hong Kong Research Grants Council (grant 11207520, to Y.L.), Medical Research Council-UK (grants MR/R013349/1 and MR/V034162/1, both to A.G.) and Research Development Fund (grant RDF-19-02-13, to J.S.) of Xi'an Jiaotong-Liverpool University.

## References

1. Bayulken B, Huisingh D, Fisher PMJ. 2021. How are nature based solutions helping in the greening of cities in the context of crises such as climate change and pandemics? A comprehensive review. *J Clean Prod* 288:125569, <https://doi.org/10.1016/j.jclepro.2020.125569>.
2. Gasparri A, Guo Y, Sera F, Vicedo-Cabrera AM, Lavigne E, Zanobetti A, Schwartz J, et al. 2015. Mortality risk attributable to high and low ambient temperature: a multi-country observational study. *Lancet* 386(9991):369–375, PMID: 26003380, [https://doi.org/10.1016/S0140-6736\(14\)62114-0](https://doi.org/10.1016/S0140-6736(14)62114-0).
3. Gasparri A, Guo Y, Sera F, Vicedo-Cabrera AM, Huber V, Tong S, et al. 2017. Projections of temperature-related excess mortality under climate change scenarios. *Lancet Planet Health* 1(9):e360–e367, PMID: 29276803, [https://doi.org/10.1016/S2542-5196\(17\)30156-0](https://doi.org/10.1016/S2542-5196(17)30156-0).
4. Zhao Q, Guo Y, Ye T, Gasparri A, Tong S, Overcenco A, et al. 2021. Global, regional, and national burden of mortality associated with non-optimal ambient temperatures from 2000 to 2019: a three-stage modelling study. *Lancet Planet Health* 5(7):e415–e425, PMID: 34245712, [https://doi.org/10.1016/S2542-5196\(21\)00081-4](https://doi.org/10.1016/S2542-5196(21)00081-4).
5. Murage P, Kovats S, Sarran C, Taylor J, McInnes R, Hajat S. 2020. What individual and neighbourhood-level factors increase the risk of heat-related mortality? A case-crossover study of over 185,000 deaths in London using high-resolution climate datasets. *Environ Int* 134:105292, PMID: 31726356, <https://doi.org/10.1016/j.envint.2019.105292>.
6. Heo S, Chen C, Kim H, Sabath B, Dominici F, Warren JL, et al. 2021. Temporal changes in associations between high temperature and hospitalizations by greenspace: analysis in the Medicare population in 40 U.S. northeast counties. *Environ Int* 156:106737, PMID: 34218185, <https://doi.org/10.1016/j.envint.2021.106737>.
7. Pascal M, Gorla S, Wagner V, Sabastia M, Guillet A, Cordeau E, et al. 2021. Greening is a promising but likely insufficient adaptation strategy to limit the health impacts of extreme heat. *Environ Int* 151:106441, PMID: 33640693, <https://doi.org/10.1016/j.envint.2021.106441>.
8. Qiu C, Ji JS, Bell ML. 2021. Effect modification of greenness on temperature–mortality relationship among older adults: a case-crossover study in China. *Environ Res* 197:111112, PMID: 33838131, <https://doi.org/10.1016/j.envres.2021.111112>.
9. Wolch JR, Byrne J, Newell JP. 2014. Urban green space, public health, and environmental justice: the challenge of making cities ‘just green enough.’ *Landsc Urban Plan* 125:234–244, <https://doi.org/10.1016/j.landurbplan.2014.01.017>.
10. Qiu GY, Li HY, Zhang QT, Chen W, Liang XJ, Li XZ. 2013. Effects of evapotranspiration on mitigation of urban temperature by vegetation and urban agriculture. *J Integr Agric* 12(8):1307–1315, [https://doi.org/10.1016/S2095-3119\(13\)60543-2](https://doi.org/10.1016/S2095-3119(13)60543-2).
11. Ng E, Chen L, Wang Y, Yuan C. 2012. A study on the cooling effects of greening in a high-density city: an experience from Hong Kong. *Build Environ* 47:256–271, <https://doi.org/10.1016/j.buildenv.2011.07.014>.
12. Diener A, Mudu P. 2021. How can vegetation protect us from air pollution? A critical review on green spaces’ mitigation abilities for air-borne particles from a public health perspective—with implications for urban planning. *Sci Total Environ* 796:148605, PMID: 34271387, <https://doi.org/10.1016/j.scitotenv.2021.148605>.
13. Margaritis E, Kang J. 2017. Relationship between green space-related morphology and noise pollution. *Ecol Indic* 72:921–933, <https://doi.org/10.1016/j.ecolind.2016.09.032>.
14. Liu L, Qu H, Ma Y, Wang K, Qu H. 2022. Restorative benefits of urban green space: physiological, psychological restoration and eye movement analysis. *J Environ Manage* 301:113930, PMID: 34731949, <https://doi.org/10.1016/j.jenvman.2021.113930>.
15. Mytton OT, Townsend N, Rutter H, Foster C. 2012. Green space and physical activity: an observational study using Health Survey for England data. *Health Place* 18(5):1034–1041, PMID: 22795498, <https://doi.org/10.1016/j.healthplace.2012.06.003>.
16. Wan C, Shen GQ, Choi S. 2021. Underlying relationships between public urban green spaces and social cohesion: a systematic literature review. *City Cult Soc* 24:100383, <https://doi.org/10.1016/j.ccs.2021.100383>.
17. Lachowycz K, Jones AP. 2013. Towards a better understanding of the relationship between greenspace and health: development of a theoretical framework. *Landsc Urban Plan* 118:62–69, <https://doi.org/10.1016/j.landurbplan.2012.10.012>.
18. Knobel P, Davdand P, Maneja-Zaragoza R. 2019. A systematic review of multi-dimensional quality assessment tools for urban green spaces. *Health Place* 59:102198, PMID: 31525616, <https://doi.org/10.1016/j.healthplace.2019.102198>.
19. Pyky R, Neuvonen M, Kangas K, Ojala A, Lanki T, Borodulin K, et al. 2019. Individual and environmental factors associated with green exercise in urban and suburban areas. *Health Place* 55:20–28, PMID: 30459052, <https://doi.org/10.1016/j.healthplace.2018.11.001>.
20. Sera F, Armstrong B, Tobias A, Vicedo-Cabrera AM, Åström C, Bell ML, et al. 2019. How urban characteristics affect vulnerability to heat and cold: a multi-country analysis. *Int J Epidemiol* 48(4):1101–1112, PMID: 30815699, <https://doi.org/10.1093/ije/dyz008>.
21. Choi HM, Lee W, Roye D, Heo S, Urban A, Entezari A, et al. 2022. Effect modification of greenness on the association between heat and mortality: a multi-city

- multi-country study. *eBioMedicine* 84:104251, PMID: 36088684, <https://doi.org/10.1016/j.ebiom.2022.104251>.
22. Madrigano J, Ito K, Johnson S, Kinney PL, Matte T. 2015. A case-only study of vulnerability to heat wave-related mortality in New York City (2000–2011). *Environ Health Perspect* 123(7):672–678, PMID: 25782056, <https://doi.org/10.1289/ehp.1408178>.
  23. Burkart K, Meier F, Schneider A, Breitner S, Canário P, Alcoforado MJ, et al. 2016. Modification of heat-related mortality in an elderly urban population by vegetation (urban green) and proximity to water (urban blue): evidence from Lisbon, Portugal. *Environ Health Perspect* 124(7):927–934, PMID: 26566198, <https://doi.org/10.1289/ehp.1409529>.
  24. Son JY, Lane KJ, Lee JT, Bell ML. 2016. Urban vegetation and heat-related mortality in Seoul, Korea. *Environ Res* 151:728–733, PMID: 27644031, <https://doi.org/10.1016/j.envres.2016.09.001>.
  25. Song J, Lu Y, Zhao Q, Zhang Y, Yang X, Chen Q, et al. 2022. Effect modifications of green space and blue space on heat–mortality association in Hong Kong, 2008–2017. *Sci Total Environ* 838(pt 2):156127, PMID: 35605868, <https://doi.org/10.1016/j.scitotenv.2022.156127>.
  26. Gascon M, Triguero-Mas M, Martínez D, Davdand P, Rojas-Rueda D, Plasència A, et al. 2016. Residential green spaces and mortality: a systematic review. *Environ Int* 86:60–67, PMID: 26540085, <https://doi.org/10.1016/j.envint.2015.10.013>.
  27. Li X, Zhang C, Li W, Ricard R, Meng Q, Zhang W. 2015. Assessing street-level urban greenery using Google Street View and a modified green view index. *Urban For Urban Green* 14(3):675–685, <https://doi.org/10.1016/j.ufug.2015.06.006>.
  28. Anguelov D, Dulong C, Filip D, Frueh C, Lafon S, Lyon R, et al. 2010. Google Street View: capturing the world at street level. *Computer* 43(6):32–38, <https://doi.org/10.1109/MC.2010.170>.
  29. Helbich M, Yao Y, Liu Y, Zhang J, Liu P, Wang R. 2019. Using deep learning to examine street view green and blue spaces and their associations with geriatric depression in Beijing, China. *Environ Int* 126:107–117, PMID: 30797100, <https://doi.org/10.1016/j.envint.2019.02.013>.
  30. Lu Y. 2019. Using Google Street View to investigate the association between street greenery and physical activity. *Landsc Urban Plan* 191:103435, <https://doi.org/10.1016/j.landurbplan.2018.08.029>.
  31. Heo S, Bell ML. 2023. Investigation on urban greenspace in relation to sociodemographic factors and health inequity based on different greenspace metrics in 3 US urban communities. *J Expo Sci Environ Epidemiol* 33(2):218–228, PMID: 35995844, <https://doi.org/10.1038/s41370-022-00468-z>.
  32. Yao Y, Xu C, Yin H, Shao L, Wang R. 2022. More visible greenspace, stronger heart? Evidence from ischaemic heart disease emergency department visits by middle-aged and older adults in Hubei, China. *Landsc Urban Plan* 224:104444, <https://doi.org/10.1016/j.landurbplan.2022.104444>.
  33. Labib SM, Huck JJ, Lindley S. 2021. Modelling and mapping eye-level greenness visibility exposure using multi-source data at high spatial resolutions. *Sci Total Environ* 755(pt 1):143050, PMID: 33129523, <https://doi.org/10.1016/j.scitotenv.2020.143050>.
  34. Zhang H, Liu L, Zeng Y, Liu M, Bi J, Ji JS. 2021. Effect of heatwaves and greenness on mortality among Chinese older adults. *Environ Pollut* 290:118009, PMID: 34523521, <https://doi.org/10.1016/j.envpol.2021.118009>.
  35. Gasparrini A. 2021. The case time series design. *Epidemiology* 32(6):829–837, PMID: 34432723, <https://doi.org/10.1097/EDE.0000000000001410>.
  36. Gasparrini A. 2022. A tutorial on the case time series design for small-area analysis. *BMC Med Res Methodol* 22(1):129, PMID: 35501713, <https://doi.org/10.1186/s12874-022-01612-x>.
  37. HKCSD (Hong Kong Census and Statistics Department). 2023. The 2016 population by-census. Last revised 15 arch 2023. <https://www.censtatd.gov.hk/en/scode459.html> [accessed 27 March 2023].
  38. Ho HC, Fong KNK, Chan TC, Shi Y. 2020. The associations between social, built and geophysical environment and age-specific dementia mortality among older adults in a high-density Asian city. *Int J Health Geogr* 19(1):53, PMID: 33276778, <https://doi.org/10.1186/s12942-020-00252-y>.
  39. Huang Z, Chan EYY, Wong CS, Zee BCY. 2022. Spatiotemporal relationship between temperature and non-accidental mortality: assessing effect modification by socioeconomic status. *Sci Total Environ* 836:155497, PMID: 35483463, <https://doi.org/10.1016/j.scitotenv.2022.155497>.
  40. HKEPD (Hong Kong Environmental Protection Department). 2023. Environmental Protection Interactive Centre: Air Quality Monitoring Data Searching Paramater. Last revised 1 September 2023. <https://cd.epic.epd.gov.hk/EPICD/air/station/?lang=en> [accessed 7 March 2023].
  41. WHO (World Health Organization). 2016. *International Statistical Classification of Diseases and Related Health Problems, 10th Revision*. <http://apps.who.int/classifications/icd10/browse/2016/en> [accessed 14 September 2023].
  42. HKCSD. 2023. The 2006 population by-census. <https://www.censtatd.gov.hk/en/scode440.html> [accessed 27 March 2023].
  43. HKCSD. 2023. Statistics: population and households. [https://www.censtatd.gov.hk/en/page\\_1226.html](https://www.censtatd.gov.hk/en/page_1226.html) [accessed 27 March 2023].
  44. Tucker CJ. 1979. Red and photographic infrared linear combinations for monitoring vegetation. *Remote Sens Environ* 8(2):127–150, [https://doi.org/10.1016/0034-4257\(79\)90013-0](https://doi.org/10.1016/0034-4257(79)90013-0).
  45. Weier J, Herring D. 2000. Measuring vegetation (NDVI & EVI). *NASA Earth Observatory*, 30 August 2000. [https://earthobservatory.nasa.gov/features/MeasuringVegetation/measuring\\_vegetation\\_1.php](https://earthobservatory.nasa.gov/features/MeasuringVegetation/measuring_vegetation_1.php) [accessed 27 March 2023].
  46. Holben BN. 1986. Characteristics of maximum-value composite images from temporal AVHRR data. *Int J Remote Sens* 7(11):1417–1434, <https://doi.org/10.1080/01431168608948945>.
  47. Zhao H, Shi J, Qi X, Wang X, Jia J. 2017. Pyramid scene parsing network. In: *2017 IEEE Conference on Computer Vision and Pattern Recognition (CVPR)*. Honolulu, HI: IEEE, 6230–6239.
  48. O'Regan AC, Hunter RF, Nyhan MM. 2021. “Biophilic cities”: quantifying the impact of Google Street View-derived greenspace exposures on socioeconomic factors and self-reported health. *Environ Sci Technol* 55(13):9063–9073, PMID: 34159777, <https://doi.org/10.1021/acs.est.1c01326>.
  49. Jimenez MP, Suel E, Rifas-Shiman SL, Hystad P, Larkin A, Hankey S, et al. 2022. Street-view greenspace exposure and objective sleep characteristics among children. *Environ Res* 214(pt 1):113744, PMID: 35760115, <https://doi.org/10.1016/j.envres.2022.113744>.
  50. Gasparrini A. 2014. Modeling exposure–lag–response associations with distributed lag non-linear models. *Stat Med* 33(5):881–899, PMID: 24027094, <https://doi.org/10.1002/sim.5963>.
  51. de Schrijver E, Royé D, Gasparrini A, Franco OH, Vicedo-Cabrera AM. 2023. Exploring vulnerability to heat and cold across urban and rural populations in Switzerland. *Environ Res Health* 1(2):025003, PMID: 36969952, <https://doi.org/10.1088/2752-5309/acab78>.
  52. Gasparrini A. 2011. Distributed lag linear and non-linear models in R: the package dlnm. *J Stat Softw* 43(8):1–20, PMID: 22003319, <https://doi.org/10.18637/jss.v043.i08>.
  53. Kilbourne EM, Choi K, Jones TS, Thacker SB. 1982. Risk factors for heatstroke. a case-control study. *JAMA* 247(24):3332–3336, PMID: 7087076, <https://doi.org/10.1001/jama.1982.03320490030031>.
  54. Xu Y, Davdand P, Barrera-Gómez J, Sartini C, Mari-Dell’Olmo M, Borrell C, et al. 2013. Differences on the effect of heat waves on mortality by sociodemographic and urban landscape characteristics. *J Epidemiol Community Health* 67(6):519–525, PMID: 23443960, <https://doi.org/10.1136/jech-2012-201899>.
  55. Uejio CK, Wilhelm OV, Golden JS, Mills DM, Gulino SP, Samenow JP. 2011. Intra-urban societal vulnerability to extreme heat: the role of heat exposure and the built environment, socioeconomic, and neighborhood stability. *Health Place* 17(2):498–507, PMID: 21216652, <https://doi.org/10.1016/j.healthplace.2010.12.005>.
  56. de Vries S, van Dillen SME, Groenewegen PP, Spreuuenberg P. 2013. Streetscape greenery and health: stress, social cohesion and physical activity as mediators. *Soc Sci Med* 94:26–33, PMID: 23931942, <https://doi.org/10.1016/j.socscimed.2013.06.030>.
  57. Lu Y, Yang Y, Sun G, Gou Z. 2019. Associations between overhead-view and eye-level urban greenness and cycling behaviors. *Cities* 88:10–18, <https://doi.org/10.1016/j.cities.2019.01.003>.
  58. Ziter CD, Pedersen EJ, Kucharik CJ, Turner MG. 2019. Scale-dependent interactions between tree canopy cover and impervious surfaces reduce daytime urban heat during summer. *Proc Natl Acad Sci USA* 116(15):7575–7580, PMID: 30910972, <https://doi.org/10.1073/pnas.1817561116>.
  59. Ho JY, Zijlema WL, Triguero-Mas M, Donaire-Gonzalez D, Valentín A, Ballester J, et al. 2021. Does surrounding greenness moderate the relationship between apparent temperature and physical activity? Findings from the PHENOTYPE project. *Environ Res* 197:110992, PMID: 33705766, <https://doi.org/10.1016/j.envres.2021.110992>.
  60. Ambrey C, Fleming C. 2014. Public greenspace and life satisfaction in urban Australia. *Urban Stud* 51(6):1290–1321, <https://doi.org/10.1177/0042098013494417>.
  61. Lo AYH, Jim CY. 2010. Differential community effects on perception and use of urban greenspaces. *Cities* 27(6):430–442, <https://doi.org/10.1016/j.cities.2010.07.001>.
  62. Jim CY, Shan X. 2013. Socioeconomic effect on perception of urban green spaces in Guangzhou, China. *Cities* 31:123–131, <https://doi.org/10.1016/j.cities.2012.06.017>.
  63. White-Newsome JL, Sánchez BN, Parker EA, Dvonch JT, Zhang Z, O’Neill MS. 2011. Assessing heat-adaptive behaviors among older, urban-dwelling adults. *Maturitas* 70(1):85–91, PMID: 21782363, <https://doi.org/10.1016/j.maturitas.2011.06.015>.
  64. Mitchell R, Popham F. 2008. Effect of exposure to natural environment on health inequalities: an observational population study. *Lancet* 372(9650):1655–1660, PMID: 18994663, [https://doi.org/10.1016/S0140-6736\(08\)61689-X](https://doi.org/10.1016/S0140-6736(08)61689-X).
  65. WGPDP (Working Group on Population Distribution Projections). 2023. Projections of Population Distribution 2021–2029. Hong Kong Planning Department. [https://www.pland.gov.hk/pland\\_en/resources/info\\_serv/statistic/wgpd21.html](https://www.pland.gov.hk/pland_en/resources/info_serv/statistic/wgpd21.html) [accessed 14 September 2023].

66. Qing Y, Wang S. 2021. Multi-decadal convection-permitting climate projections for China's Greater Bay Area and surroundings. *Clim Dyn* 57(1–2):415–434, <https://doi.org/10.1007/s00382-021-05716-w>.
67. de Vries S, Verheij RA, Groenewegen PP, Spreeuwenberg P. 2003. Natural environments—healthy environments? An exploratory analysis of the relationship between greenspace and health. *Environ Plan A* 35(10):1717–1731, <https://doi.org/10.1068/a35111>.
68. Thompson R, Hornigold R, Page L, Waite T. 2018. Associations between high ambient temperatures and heat waves with mental health outcomes: a systematic review. *Public Health* 161:171–191, PMID: 30007545, <https://doi.org/10.1016/j.puhe.2018.06.008>.
69. Fernández Núñez MB, Campos Suzman L, Maneja R, Bach A, Marquet O, Anguelovski I, et al. 2022. Gender and sex differences in urban greenness' mental health benefits: a systematic review. *Health Place* 76:102864, PMID: 35853366, <https://doi.org/10.1016/j.healthplace.2022.102864>.
70. Son JY, Liu JC, Bell ML. 2019. Temperature-related mortality: a systematic review and investigation of effect modifiers. *Environ Res Lett* 14(7):073004, <https://doi.org/10.1088/1748-9326/ab1cdb>.
71. Sorensen C, Murray V, Lemery J, Balbus J. 2018. Climate change and women's health: impacts and policy directions. *PLoS Med* 15(7):e1002603, PMID: 29990343, <https://doi.org/10.1371/journal.pmed.1002603>.
72. Yang J, Zhou M, Ren Z, Li M, Wang B, Liu DL, et al. 2021. Projecting heat-related excess mortality under climate change scenarios in China. *Nat Commun* 12(1):1039, PMID: 33589602, <https://doi.org/10.1038/s41467-021-21305-1>.
73. Wu J, Rappazzo KM, Simpson RJ Jr, Joodi G, Pursell IW, Mounsey JP, et al. 2018. Exploring links between greenspace and sudden unexpected death: a spatial analysis. *Environ Int* 113:114–121, PMID: 29421400, <https://doi.org/10.1016/j.envint.2018.01.021>.
74. Piel FB, Fecht D, Hodgson S, Blangiardo M, Toledano M, Hansell AL, et al. 2020. Small-area methods for investigation of environment and health. *Int J Epidemiol* 49(2):686–699, PMID: 32182344, <https://doi.org/10.1093/ije/dyaa006>.
75. Jimenez RB, Lane KJ, Hutyra LR, Fabian MP. 2022. Spatial resolution of normalized difference vegetation index and greenness exposure misclassification in an urban cohort. *J Expo Sci Environ Epidemiol* 32(2):213–222, PMID: 35094014, <https://doi.org/10.1038/s41370-022-00409-w>.
76. Fong KC, Hart JE, James P. 2018. A review of epidemiologic studies on greenness and health: updated literature through 2017. *Curr Environ Health Rep* 5(1):77–87, PMID: 29392643, <https://doi.org/10.1007/s40572-018-0179-y>.
77. Twohig-Bennett C, Jones A. 2018. The health benefits of the great outdoors: a systematic review and meta-analysis of greenspace exposure and health outcomes. *Environ Res* 166:628–637, PMID: 29982151, <https://doi.org/10.1016/j.envres.2018.06.030>.
78. He Y, Cheng L, Bao J, Deng S, Liao W, Wang Q, et al. 2020. Geographical disparities in the impacts of heat on diabetes mortality and the protective role of greenness in Thailand: a nationwide case-crossover analysis. *Sci Total Environ* 711:135098, PMID: 32000339, <https://doi.org/10.1016/j.scitotenv.2019.135098>.
79. Rugel EJ, Henderson SB, Carpiano RM, Brauer M. 2017. Beyond the normalized difference vegetation index (NDVI): developing a natural space index for population-level health research. *Environ Res* 159:474–483, PMID: 28863302, <https://doi.org/10.1016/j.envres.2017.08.033>.
80. Helbich M. 2018. Toward dynamic urban environmental exposure assessments in mental health research. *Environ Res* 161:129–135, PMID: 29136521, <https://doi.org/10.1016/j.envres.2017.11.006>.
81. Sadeh M, Brauer M, Dankner R, Fulman N, Chudnovsky A. 2021. Remote sensing metrics to assess exposure to residential greenness in epidemiological studies: a population case study from the Eastern Mediterranean. *Environ Int* 146:106270, PMID: 33276312, <https://doi.org/10.1016/j.envint.2020.106270>.
82. Wang R, Helbich M, Yao Y, Zhang J, Liu P, Yuan Y, et al. 2019. Urban greenery and mental wellbeing in adults: cross-sectional mediation analyses on multiple pathways across different greenery measures. *Environ Res* 176:108535, PMID: 31260914, <https://doi.org/10.1016/j.envres.2019.108535>.
83. Buckley JP, Samet JM, Richardson DB. 2014. Commentary: does air pollution confound studies of temperature? *Epidemiology* 25(2):242–245, PMID: 24487206, <https://doi.org/10.1097/EDE.0000000000000051>.